# Two Light-Activated Conductances in the Eye of the Green Alga *Volvox carteri*

Franz-Josef Braun and Peter Hegemann
Institut für Biochemie I, Universität Regensburg, 93040 Regensburg, Germany

ABSTRACT Photoreceptor currents of the multicellular green alga *Volvox carteri* were analyzed using a dissolver mutant. The photocurrents are restricted to the eyespot region of somatic cells. Photocurrents are detectable from intact cells and excised eyes. The rhodopsin action spectrum suggests that the currents are induced by *Volvox* rhodopsin. Flash-induced photocurrents are a composition of a fast $Ca^{2+}$-carried current ($P_F$) and a slower current ($P_S$), which is carried by $H^+$. $P_F$ is a high-intensity response that appears with a delay of less than 50 $\mu$s after flash. The stimulus-response curve of its initial rise is fit by a single exponential and parallels the rhodopsin bleaching. These two observations suggest that the responsible channel is closely connected to the rhodopsin, both forming a tight complex. At low flash energies $P_S$ is dominating. The current delay increases up to 10 ms, and the $P_S$ amplitude saturates when only a few percent of the rhodopsin is bleached. The data are in favor of a second signaling system, which includes a signal transducer mediating between rhodopsin and the channel. We present a model of how different modes of signal transduction are accomplished in this alga under different light conditions.

## INTRODUCTION

*Volvox carteri* is a spherical multicellular alga with many features that recommend it as a model for studying the process of cytodifferentiation (Kirk and Harper, 1986) and the early development of photoreception in eucaryotes. Individuals of this species contain only two distinct cell types, 16 large reproductive cells (gonidia) and 2000–4000 somatic cells that cannot divide. The somatic cells are arranged in a single layer at the surface of the transparent sphere, whereas the 16 gonidia are located below the surface, where they have no direct contact with the external medium (Fig. 1; Kirk et al., 1991). All somatic cells are flagellated and possess eyes, and they are responsible for guiding the colony to places of light conditions that are optimal for photosynthetic growth. The orientation of the individual somatic cells within the spheroid, combined with the three-dimensional pattern in which their flagella beat, cause the spheroid to rotate in a counterclockwise direction (as seen along the swimming vector; Hoops, 1993). The two flagella of each cell beat synchronously and in an almost precisely parallel fashion. The flagella of all cells beat toward the posterior of the spheroid and slightly to the right, causing the spheroid to rotate to the left as it moves forward (Hoops, 1993, 1997). Anterior cells possess larger and more sensitive eyes than posterior ones (Sakaguchi and Iwasa, 1979; Hoops, 1997). In *Volvox* the photophobic response involves a cessation of flagellar movement, and not a switch to a different beating mode of the sort that causes slow backward movement in most of its unicellular relatives. When a *Volvox* spheroid is illuminated from one side, its rotation causes the cells to pass repeatedly between the shaded and the lit sides, with the consequence that their flagella slow down or accelerate beating, turning the colony either toward or away from the light (Foster and Smyth, 1980). Whether cells accelerate or decelerate in response to on and off stimuli depends on the light intensity and its illumination history. Thus, in other words, colonial algae orient in light by a complex differential response of the cells at different sides of the colony and not by a differential response of the two flagella in an individual cell. Because algal colonies rotate more slowly than single-cell species, light-mediated signaling in an alga that exists in colonies is also expected to be slower than signaling in a single-celled alga.

All light-induced behavioral responses show action spectra with maxima between 490 and 520 nm (Schletz, 1976; Sakaguchi and Iwasa, 1979), suggesting that in *Volvox* a rhodopsin similar to the chlamyrhodopsin of its unicellular relative *Chlamydomonas reinhardtii* (Deininger et al., 1995) serves as the functional photoreceptor for behavioral light responses. A volvoxopsin gene (*vop*) with striking homology to the chlamyopsin sequence (*cop*) was recently identified (Ebnet et al., manuscript submitted for publication).

We present the first measurements of photoreceptor currents produced by somatic cells of the colony-forming alga *V. carteri*. Because all cells of the wild-type colony are enclosed in a complex extracellular matrix that precludes this kind of electrophysiological measurement, the studies were performed with a "dissolver" mutant of *V. carteri* that develops as a suspension of single cells that are substantially free of such a matrix. Photocurrents were recorded from intact cells and excised eyes in response to short flashes or longer light pulses under various ionic conditions. All recorded photocurrents are well explained by two inde-

*Received for publication 2 June 1998 and in final form 18 November 1998.*
Address reprint requests to Dr. Peter Hegemann, Institut für Biochemie I, Universität Regensburg, 93040 Regensburg, Germany. Tel.: 0049-941-943-2814; Fax: 0049-941-943-2936; E-mail: peter.hegemann@biologie.uni-regensburg.de. http://www.biologie.uni-regensburg.de/Biochemie/Hegemann

0006-3495/99/03/1668/11 $2.00

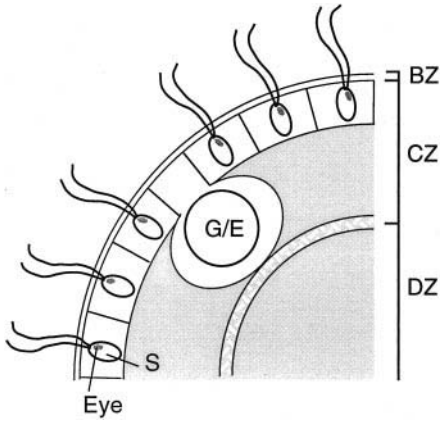


FIGURE 1 The two cell types in *Volvox carteri*. Schematized arrangement of somatic cells (S) and gonidia or the embryos derived from the gonidia (G/E) within a *Volvox* wild-type colony. Somatic cells and gonidia are embedded in the cellular zone (CZ), whereas the deep zone (DZ) and boundary zone (BZ) are free of cells (Kirk et al., 1986).

pendent conductances that are localized within the eyespot area.

## MATERIALS AND METHODS

### Description of the *Volvox* mutant used for photocurrent recording

In a wild-type *V. carteri* spheroid, all cells are enclosed in a complex extracellular matrix that surrounds all cells and holds them in fixed relationship to one another (Fig. 1). Therefore our electrical studies were performed with a "dissolver" mutant that develops as a suspension of single cells free of extracellular matrix (ECM). The dissolver strain used here (W251) ($gls^-/regA^-/dis^-$) arose as a spontaneous mutant in a culture of a previously described "gonidia-less/regenerator" strain (Tam and Kirk, 1991) and was provided to us by Dr. D. Kirk (St. Louis, MO). In wild-type *V. carteri* there is a complete division of labor in which the biflagellate somatic cells are specialized for motility and are incapable of dividing, whereas the gonidia are specialized for reproduction and never have functional flagella. In the Gls/Reg strain, however, this division of labor is abolished by two mutations ($gls^-$ and $regA^-$): all cells of a Gls/Reg mutant first develop as biflagellate cells that are indistinguishable from wild-type somatic cells in their phototactic activity; then a day later they all dedifferentiate (resorbing their flagella and eyespots) and redifferentiate as gonidia that will divide to produce progeny of like phenotype. With the addition of a third mutation ($dis^-$) that interferes with the production of the extracellular matrix (ECM), which normally functions to hold the cells together after they completed embryogenesis, the W251 (Dis/Gls/Reg) strain develops as a uniform population of cells that separate from one another at the end of embryogenesis. These individuals first develop as somatic cells with flagella and eyespots and later differentiate as eye- and flagella-less gonidia. The W251 mutant was grown synchronized under a 16h/8h light-dark regime (14 $Wm^{-2}$) in standard medium (Provasoli and Pinter, 1959) at 28°C.

### Electrical measurements

For electrical measurements cells of the mutant strain W251 were centrifuged at 3000 rpm and resuspended in $NMG^+/K^+$ buffer (5 mM HEPES, 10 mM $Cl^-$, 1 mM $K^+$, 200 $\mu$M 1,2-bis(2-aminophenoxy)ethane-*N,N,N,N*-tetraacetic acid, 300 $\mu$M $Ca^{2+}$, adjusted with *N*-methyl-D-glucamine (NMG) to pH 6.8). After dark adaptation for more than 1 h, cells were used for experiments. The $NMG^+/K^+$ buffer was used as the electrode and bath solution. $Ca^{2+}$ was added as $CaCl_2$. The total $Ca^{2+}$ concentration required for a defined concentration of free $Ca^{2+}$ was calculated according to the method of Holland et al. (1996).

### Suction pipette measurements

Photocurrents were recorded by using borosilicate suction pipettes with a final tip diameter in the range of one-half of the cell diameter (i.d.) (Harz et al., 1992; Holland et al., 1996). The pipettes had an access resistance of 20–50 MΩ. Cells were sucked into the pipette by up to one-half until the resistance reached 60–150 MΩ. Under these experimental conditions, one-third of the total current can be detected under the capacitive mode (for further explanation see Holland et al., 1996). Currents were recorded at constant voltage (0 mV between bath and pipette) and were filtered with a 3-kHz low-pass Bessel filter. Data were recorded and processed as described by Harz et al. (1992). If not otherwise indicated, the current traces shown are the mean of 7–10 individual recordings filtered with a digital Gaussian filter to 500 Hz. The orientation of the cells was not optimized for maximum light sensitivity as described before by Harz et al. (1992).

### Patch pipette measurements

Pipettes for measuring P-currents directly at the eyespot were pulled from borosilicate glass capillaries (1.8-mm outer diameter, 0.15-mm walls, Kimax-51; Witz Scientific, Maumee, OH) in two steps and were polished until the tip diameter reached ~1.5 $\mu$m. The cone angle was ~30°. The pipettes were filled and currents were measured in $NMG^+/K^+$ buffer. The resistance of the pipette was 15–20 MΩ. When the eye (diameter 1.5 $\mu$m) was sucked into the pipette, the resistance increased to 120–160 MΩ. A 40× objective (NA = 1.3; Achrostigmat, Zeiss) and a 4× phototube were used for identifying the eyespot in infrared light on the screen. Starting from this configuration, eyespot vesicles were prepared. While low pressure was applied to the eye in the pipette, the major part of the cell was cut off with a second pipette (see Fig. 5). The remaining eyespot vesicle was pressed against the pipette tip by applying weak pressure to create an acceptable seal resistance (120 MΩ). The eyeless cell was kept in the second pipette for control experiments. Currents were filtered with a 10-kHz low-pass Bessel filter and recorded with a frequency of 100 kHz.

The cells or vesicles were stimulated through the objective by a 10-$\mu$s flash (IG&G FXQG-949-1; Polytech, Waldbronn). One hundred percent photon exposure (500 nm, 60 nm half-bandwidth) corresponds to $2.6 \times 10^{20}$ photons $m^{-2}$ in the objective plane. Light pulses of 500 ms were applied with a 75-W xenon lamp, and the duration was controlled with a fast electronic shutter (Uniblitz model T132; Vincent Associates, Rochester, NY). One hundred percent photon irradiance (500 nm, 60 nm half-b.w.) corresponds to $1 \times 10^{21}$ photons $m^{-2}$ $s^{-1}$.

If not otherwise indicated, the measurements were carried out at room temperature (20°C).

## RESULTS

The Dis/Gls/Reg strain, used in all electrical measurements described below, provided two advantages. First, it produced biflagellate somatic cells that could easily be drawn into a suction pipette. The cell surfaces are sufficiently free of extracellular matrix (ECM) that photoreceptor currents were readily examined and characterized. Second, the ability of these somatic cells to redifferentiate as eyeless gonidia provided us an opportunity to determine whether the gonidia continue to produce photocurrents after they have lost their visible eyespots, which are known to serve as an optical system (Foster and Smyth, 1980).

### Recording photocurrents from the Dis/Gls/Reg mutant

To track down rhodopsin-mediated electrical events, small somatic cells with a diameter of 8 $\mu$m were sucked into the suction pipette with flagella and eyes outside the pipette and were stimulated with bright green flashes ($>10^{20}$ photons $m^{-2}$). Transient photocurrents with a peak amplitude of up to 12 pA appeared (fast photoreceptor current, $P_F$, in Fig. 2 *a*). The photocurrents peaked at ~2.5 ms after the flash and decayed with $\tau$ in the range of 12 ms to a new plateau. The current finally decayed within 0.5–1 s (slow photoreceptor current, $P_S$). Photocurrents recorded from larger *Volvox* cells with diameters of 10–16 $\mu$m had a very similar peak amplitude (Fig. 2 *b*). Only the decay was slightly retarded. The $\tau$ values and the integrals increased up to 1.6-fold. When the cells reached diameters above 20 $\mu$m, the eyespot pigmentation disappeared and the cells turned into gonidia and began to divide. Independent of the number of divisions completed, neither the gonidia nor their daughter cells exhibited any photocurrents (Fig. 2 *c*). Apparently, the electrical photoresponsiveness became totally inactivated during conversion into gonidia within a time range of 2–3 h. Such an abrupt, developmentally controlled inactivation of a visual process has not been observed, to our knowledge, in any other organism.

### Light dependence of the P-currents and evidence for its activation by rhodopsin

The photocurrents recorded from the somatic cells are all confined to the eyespot region. The photocurrents had a positive sign under our measuring conditions whenever the eyespot was outside the pipette, and there was an inward current from the bath into the eyespot (Fig. 3 *a*). When the eyespot was in the pipette, the inward current from the pipette into the eye was monitered, and the whole current inverted to negative (Fig. 3 *b*; Harz et al., 1992; Holland et al., 1996), indicating that all current components are localized within the eyespot area. It is expected that the P-currents are larger when measured with the eyespot in the pipette compared to recordings with the eyespot outside, because a large fraction of the total current is detected. However, this was not the case, because the eyespot was in most experiments pressed against the pipette wall and was not freely accessible. The kinetic features of the currents were identical in the two eyespot orientations. The kinetics of the maximum response, shown in Fig. 3 *b*, were determined as $\tau_1 = 1.0$ ms, $\tau_2 = 12.7$ ms, and $\tau_3 = 76.4$ ms. $P_F$ was graded with the photon exposure (Fig. 3, *a* and *b*). To study photocurrents at low photon exposure, we used patch pipettes with a small tip diameter and a steep cone angle (Fig. 3 *c*). This configuration improved the resolution and allowed us to record photocurrents of less than 0.2 pA. The stimulus-response curve of the $P_F$ peak covered a dynamic range of almost four log units of photon exposure (Fig. 3 *c*). The slope was too small to be fit by an exponential or by a hyperbolic saturation curve.

To study $P_F$ independently of the $P_S$, the trace recorded at 3% photon exposure (Fig. 3 *b*), where only a small fraction of the rhodopsin is bleached, was substracted from the traces recorded at higher flash energies. The residual currents were normalized; these are shown in Fig. 3 *d*. The rise, the peak time, and the decay of these residuals were almost constant for every cell and independent of the current size. The decay was now described by a single exponential, and the $\tau$-value was close to $\tau_2$ of the total current shown in Fig. 3 *b*. Because of the increasing amplitude and the constant decay, the current integral is graded with the photon exposure (Fig. 3 *e*), and because the cell is almost at isopotential, the degree of depolarization should change accordingly (Harz et al., 1992). The depolarization must be smaller in larger cells because the P-current integral does not increase in parallel with the cell surface area. The invarability of the $P_F$ time constants is a clear difference from *Chlamydomonas*, where P-currents with large amplitude decay faster than smaller currents, leaving the P-current integral and the degree of depolarization rather constant between 10% and 100% receptor bleaching (Fig. 3 *e*).

The linear part of the $P_F$ stimulus-response curve was determined at five different wavelengths. After the curves were extrapolated to zero, the threshold sensitivities were plotted as a function of photon energy (Fig. 3 *f*). The action spectrum peaked at 495 nm (2.51 eV). The close fit of the spectrum to a rhodopsin standard curve on one hand and to the action spectrum for rhodopsin-triggered photocurrents in *Chlamydomonas* on the other hand leaves little doubt that the photoreceptor is a rhodopsin. The spectrum matches, as expected, the low-intensity action spectrum for phototaxis, whereas the high-intensity phototaxis spectrum is finely

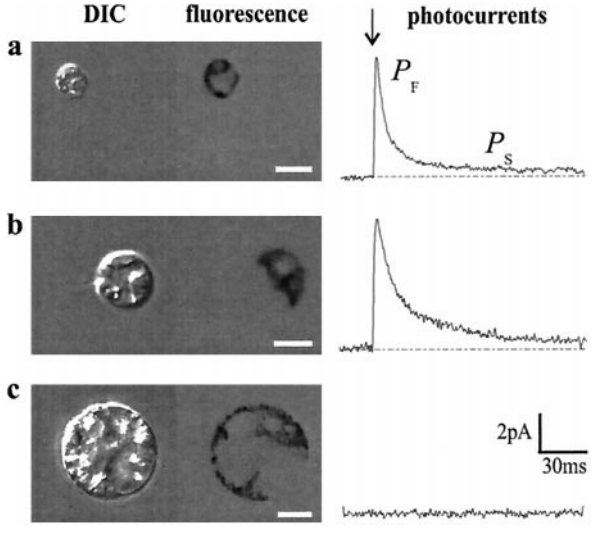


FIGURE 2 Cell specificity of the photocurrents. Normarski images (DIC), chlorophyll fluorescence, and flash-induced photocurrents ($P_F$ and $P_S$) were recorded from strain W251 small and large somatic cells (*a* and *b*) and from a reproductive cell (gonidium) after first division (*c*). Currents were recorded from somatic cells with eyespot and flagella outside the pipette. Bar = 10 $\mu$m.

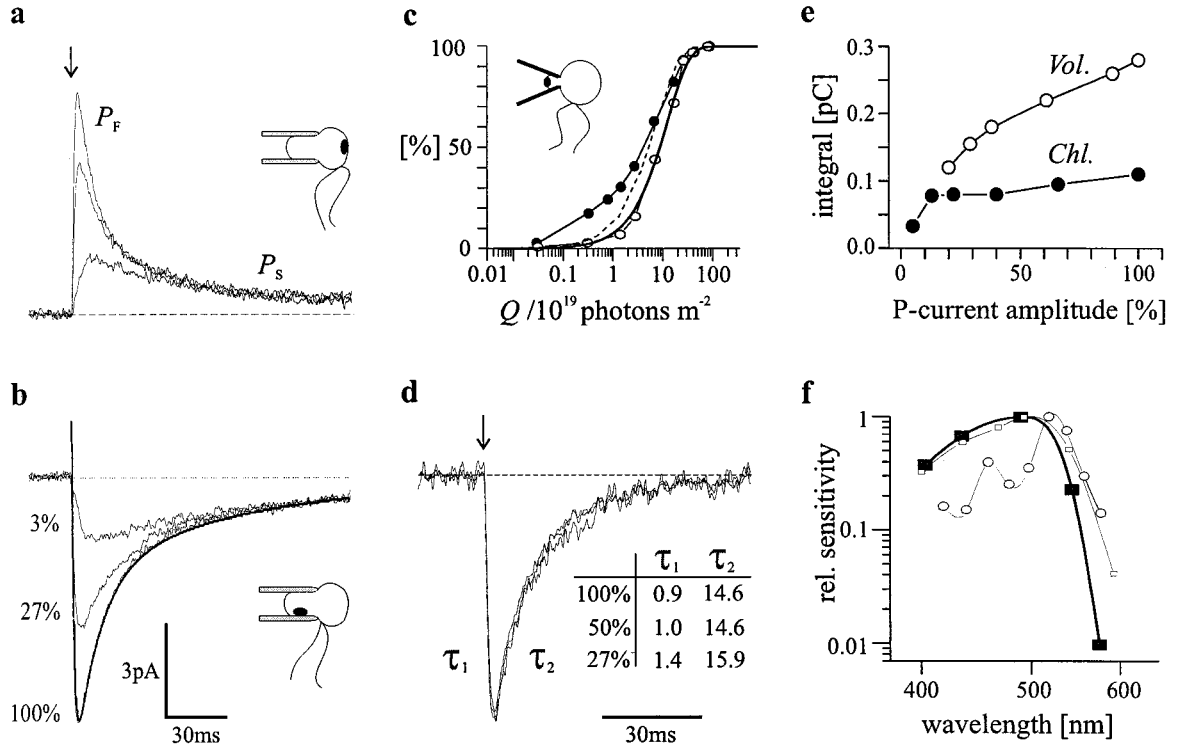


FIGURE 3 Light dependence. (*a* and *b*) Flash-induced fast ($P_F$) and slow ($P_S$) photoreceptor currents recorded with a suction pipette from somatic cells with eyespots outside (*a*) or inside (*b*) the pipette. A 100% flash corresponds to a photon exposure of $2.6 \times 10^{20}$ photons $m^{-2}$. The solid line in *b* represents a fit. The rise is monoexponential ($\tau_1 = 1.0$ ms), whereas the decay is biexponential ($\tau_2 = 12.7$ ms and $\tau_3 = 76.4$ ms). (*c*) Stimulus-response curves of normalized $P_F$ peak amplitudes (●) and the linear phase of the current rise (○). Each data point represents the average of seven recordings. The dashed line shows a saturation curve calculated according to Eq. 1. The solid line is the curve fitting according to Eq. 1. (*d*) Normalized $P_F$ currents recorded at 100%, 50%, and 27% photon exposure from the same cell after substraction of the 3% trace shown under *b*. (*e*) Plot of the *Volvox* $P_F$ integral versus the normalized $P_F$ amplitude (○) in comparison with integrals of the *P* current recorded from a *Chlamydomonas* cell (strain CW2) of the same size (●). (*f*) Action spectrum of the $P_F$ current recorded with patch pipettes directly from the eye (■) in comparison with a published low-intensity action spectrum for photophobic responses (□) (data taken from Schletz, 1976) and a high-intensity spectrum of the same response (○) (data from Sakaguchi and Iwasa, 1979) of wild-type *Volvox carteri* colonies. The data points of the $P_F$ spectrum are averaged values of four cells.

structured (Fig. 3 *f*). The shape of the photocurrent action spectrum and its location on the energy scale exclude the contribution of phytochrome as well as flavin-based light receptors (Smyth et al., 1988).

The cells did not exhibit any action potential like flagellar currents, $F_F$, which is a great benefit for the analysis of the photoreceptor currents. In single-celled algae $F_F$ overlaps with the P-current and distorts the measured decay at high flash energies (Litvin et al., 1978; Harz and Hegemann, 1991).

## The light dependence of the P-current rise

In flash experiments the P-current rise was determined by extrapolating its linear part to zero (Fig. 4 *a*, *inset*). The rise increases with the photon exposure, and its stimulus-response curve is fit by a single exponential function quite adequately (Fig. 3 *c*). An exponential light dependence is expected if the fraction of channels activated and the number of charges entering the cell per time unit are proportional to the photon exposure until all rhodopsin is bleached. The simplest explanation is a constant ratio between actived receptor molecules and the number of activated channels:

$$P/P_{max} = 1 - e^{-Qk} \quad (1)$$

where $P$ is the number of channels activated, and $Q$ is the amount of light absorbed (photon exposure) (Lamb et al., 1981). A hyperbolic saturation curve, $Qk/(1 + Qk)$, describes the experimental data less accurately, even if a Hill coefficient is included (data not shown). Substituting in Eq. 1 the constant $k$ for the product of a typical rhodopsin absorption cross section $\sigma = 1.9 \times 10^{-20}$ $m^2$ times the rhodopsin quantum efficiency of $\varphi = 0.67$, numerical values were calculated. This calculated saturation curve is shifted to lower flash energies by only a factor of 2 relative to the experimental data.

In *Volvox*, the $P_F$ induced by an intense flash of 10 $\mu$s duration and a photon exposure between $10^{19}$ and $10^{20}$ photons $m^{-2}$ begins to rise with virtually no delay (below 50 $\mu$s; Fig. 4 *a*), which closely resembles the rapid P-current rise in *Haematococcus* and *Chlamydomonas* (Sineshchekov et al., 1990; Holland et al., 1996). This immediate channel

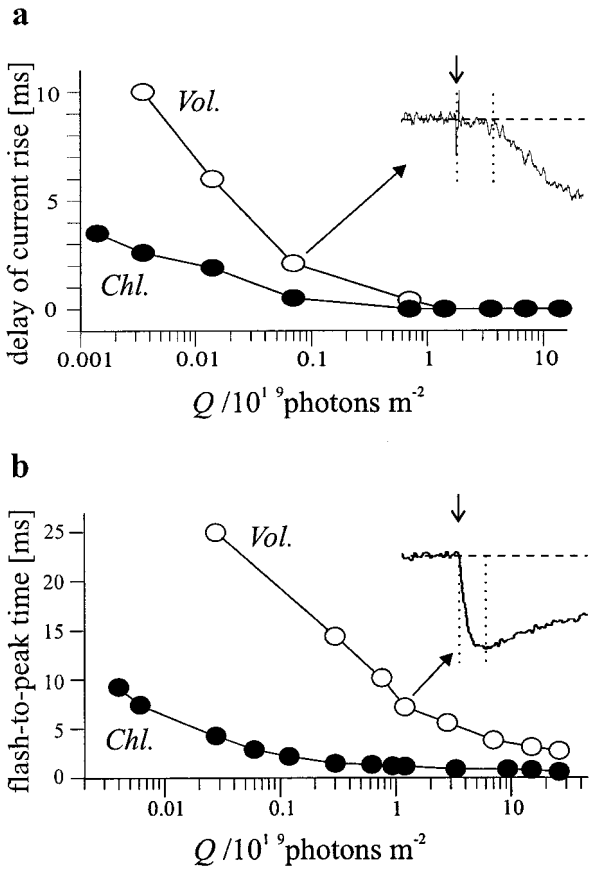


FIGURE 4 Delay and flash-to-peak time. (*a*) The delay between flash and beginning of the *Volvox P* current is plotted versus log photon exposure (○). The delay of the *P* current of the unicellular alga *Chlamydomonas* was measured under identical conditions and plotted for comparison (●) (averages of 50 individual recordings, 100-kHz sampling, 10-kHz low-pass filter, 10-kHz Gauss filter). (*b*) The flash to peak time is plotted versus log photon exposure (averages of 10 individual recordings, 10-kHz low-pass filter, 1-kHz Gauss filter). All traces were measured with an eyespot inside a small patch pipette. The insets show representative responses to flashes of the indicated energies. The arrows in the insets mark the time of the flash.

activation led to the suggestion that the rhodopsin and the photoreceptor channel in microalgae are in close contact or even form one functional complex (Harz et al., 1992). Now, because of the improved signal resolution, the *Volvox* P-currents were measured down to flash energies of only $10^{16}$ photons $m^{-2}$, where only a small fraction of rhodopsin molecules (0.01%) are activated. At this low photon exposure the current rises in a sigmoidal fashion. The delay, also defined by extrapolating the linear part of the curve to zero (Fig. 4 *a*, *inset*), increases dramatically at low photon exposure, reaching in *Volvox* values up to 10 ms when only a total of few photons are absorbed (Fig. 4 *a*). The flash-to-peak time is extended accordingly from 2.5 and 25 ms (Fig. 4 *b*). In contrast to the delay, the variability of the flash-to-peak time is detectable up to light saturation. It is well explained solely by the light dependence of the rise shown in Fig. 3 *c*. Both the $P_F$ delay and the flash-to-peak time are larger than their counterparts in *Chlamydomonas*, which are plotted for comparison in Fig. 4.

## Photocurrents recorded from excised eyes

When the *Volvox* cells are sucked into small patch pipettes and strong underpressure is applied, vesicles are sometimes pulled off into the pipette. Better control of the vesicle size is achieved by pinching them off mechanically with the help of a suction pipette (Fig. 5 *a*). Photocurrents could be recorded from those amputated cells that still contained the eye. Proportionally to the size reduction of the cell, both P-currents were reduced in their amplitude (Fig. 5 *b*). However, the kinetics of the P-current, the time of the current maximum (Fig. 5 *c*), and the light sensitivity of the cell (not shown) were left unchanged. Finally, photocurrents were recorded from vesicles that contained only the eyespot and very little of the residual cell (Fig. 5 *b*). These small vesicles had to be pressed against the inside of the pipette outlet to produce the same electrical resistance as with intact cells. The amplitude of the P-currents was in the range of only

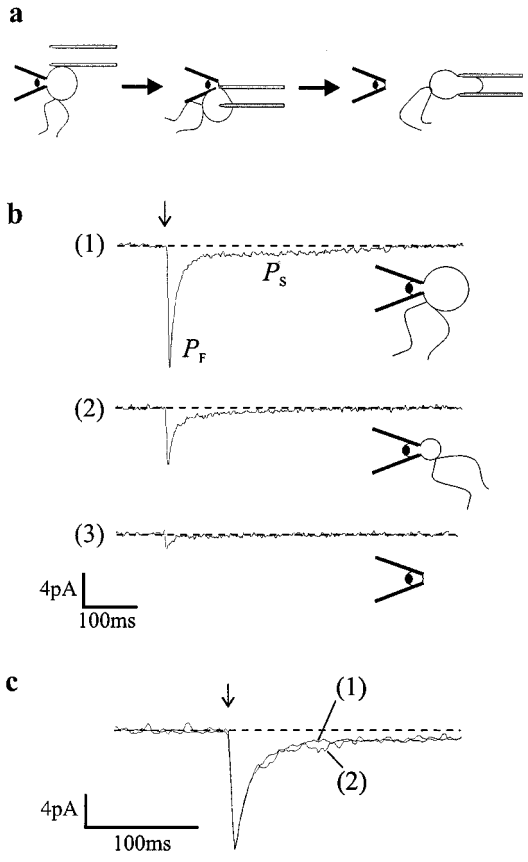


FIGURE 5 Photocurrents from eyespot vesicles. (*a*) Preparation. After shearing of the major part of the cell with a suction pipette, the eyeless residual cell was kept in the suction pipette, whereas the eye vesicle remained in the patch pipette. (*b*) Photocurrents recorded from intact cells (*1*), from cells with reduced volume (*2*), and from a small eye-containing vesicle (*3*) (photon exposure: $2.6 \times 10^{20}$ photons $m^{-2}$). Eyeless cells were unresponsive to light. (*c*) Normalized currents taken from *b*, *1* and *2*.

10% of the currents recorded from intact cells, but all other properties were again left unchanged. The reason for the size reduction is unclear, but certainly the seal between pipette and vesicle contributes to a larger extent to the total resistance, and it is conceivable that the membrane potential of the vesicle is less negative than that of the intact cell. Cells with no eyes were totally insensitive to light stimulation. These experiments provide the most direct proof so far that the receptor and the signal transduction system *Volvocales* are located within the eyespot area.

### The slow photoreceptor current, $P_S$

As seen in Figs. 2, 3 and 5, the $P_F$ is followed by a second current component that decays only slowly. The light dependence of this $P_S$ is different from that of the $P_F$ current. Its amplitude under physiological conditions (200 $\mu$M $Ca^{2+}$, 1 mM $K^+$, pH 7) is only 0.5–1 pA, with little change over a range of two orders of photon exposure (Fig. 6 *a*). In other words, it is already saturated when only a few percent of the photoreceptor is bleached. It should be kept in mind that this relationship is independent of the number of photoreceptors per cell. In contrast, the duration of $P_S$ continuously increases with the photon exposure in a dose-dependent manner (Fig. 6 *b*), i.e., when more receptor is bleached the duration but not its size increases.

### The stationary photoreceptor current, $P_{St}$

Because the natural stimulus of a *Volvox* colony is modulated continuous light instead of short flashes, in a separate set of experiments light pulses with a duration in the second range were applied to small somatic cells. Besides the transient $P_F$ current, a stationary current appeared and continued as long as the light was kept on (at least for 20 s) (Fig. 7 *a*). Modulation of the photon irradiance during the light period modulated the amplitude of the stationary current accordingly (data not shown). The current sign inverted from positive to negative when the eye was sucked into the pipette (as seen in Fig. 7 *a*), independent of the location of the flagella. Because this sign inversion indicates the eyespot location, the stationary current is again an eye-specific current and was termed $P_{St}$. The $P_{St}$ amplitude saturates at low photon irradiance (Fig. 7 *b*) in a way similar to that of the peak amplitude of $P_S$. $P_F$ only appeared when $P_{St}$ nearly saturated. After the light was turned off, $P_{St}$ decayed with a time constant $\tau$ of around 150 ms, independent of the former light intensity.

### $Ca^{2+}$, $H^+$, and $K^+$ dependence of the *P* currents

The photocurrents depend in a distinctive way on the extracellular ion composition. Lowering the extracellular $Ca^{2+}$ below 10 nM in flash experiments led to a disappearence of the transient $P_F$ within 1 min, whereas $P_S$ remained unchanged. $P_F$ immediately reappeared when

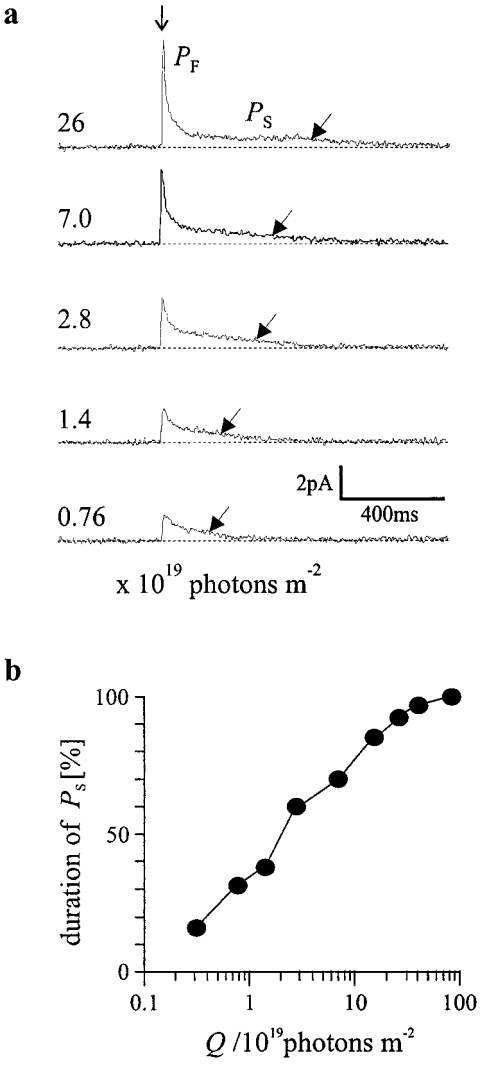


FIGURE 6 The slow photoreceptor current $P_S$. (*a*) Light dependence of the *P* currents, with emphasis on slow $P_S$ current duration. Arrows indicate when $P_S$ falls below 0.5 pA. (*b*) The duration of $P_S$ plotted versus log photon exposure.

$Ca^{2+}$ was readded and the flashing was continued (Fig. 8 *a*). Apparently, under physiological conditions $P_F$ is mainly carried by $Ca^{2+}$, whereas the $P_S$ is $Ca^{2+}$-independent. $Ba^{2+}$ substitutes for $Ca^{2+}$ ions with unchanged kinetics, suggesting that $Ca^{2+}$-regulated intracellular processes are not involved. At 200 $\mu$M $Ca^{2+}$, the addition of 1 mM $La^{3+}$ led to a total disappearence of all electrical light responses. The stationary current, $P_{St}$, is not dominated by $Ca^{2+}$ but shows some $Ca^{2+}$ dependence. Its size varied by less than a factor of 2 when the extracellular $Ca^{2+}$ concentration was varied between 10 nM and 200 $\mu$M (Fig. 8 *b*). Thus a $Ca^{2+}$ conductance might contribute to $P_{St}$ as in animal photoreceptor currents, but it is certainly not the major current carrier.

All three currents, $P_F$, $P_S$, and $P_{St}$, are profoundly affected by the extracellular pH. At acidic pH both $P_F$ and $P_S$ dramatically increase in size, suggesting that both currents are mainly carried by $H^+$ under these conditions (Fig. 8 *c*).

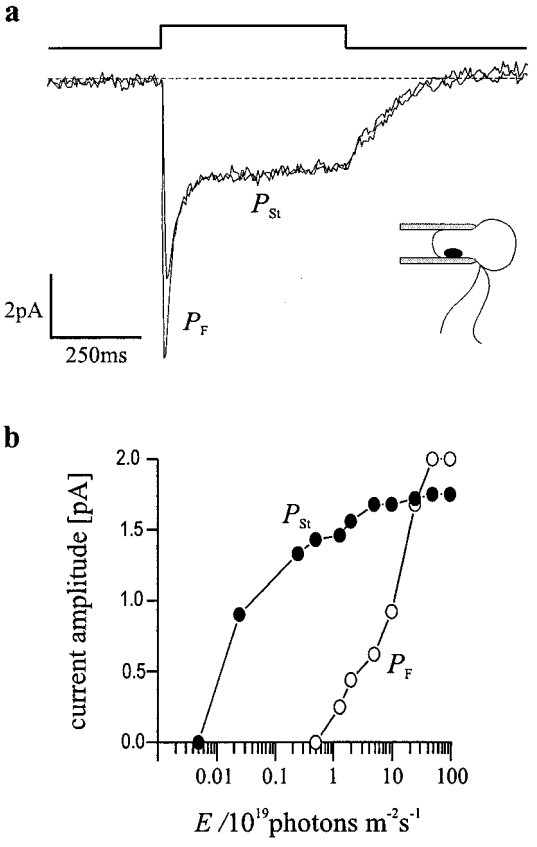


FIGURE 7 Stationary photocurrents. (*a*) Photocurrents in response to a light pulse (100% and 25%) with the eyespot inside and flagella outside the pipette. The duration of the light pulse is indicated above the current traces (12 averages, digital Gaussian filter 100 Hz). (*b*) The amplitudes of $P_F$ and $P_{St}$ are plotted versus log photon irradiance (mean values from five cells).

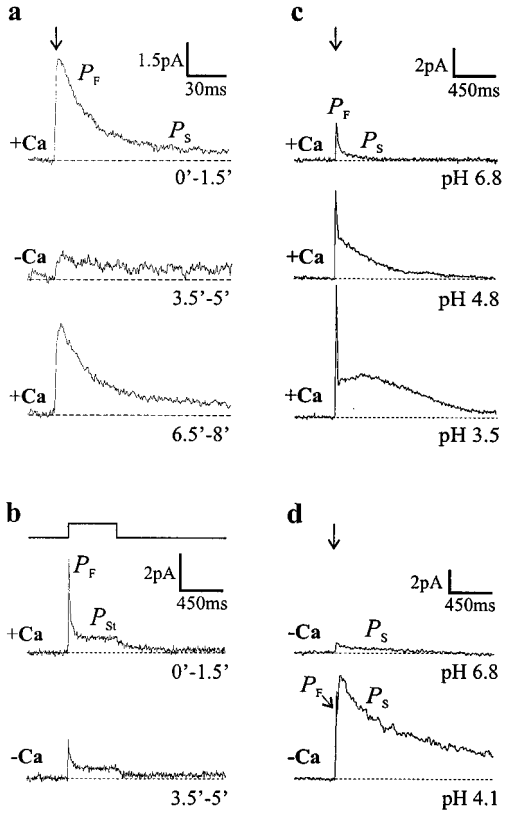


FIGURE 8 $Ca^{2+}$ and pH dependence. (*a* and *b*) Suppression of the $P_F$ current upon reduction of $Ca^{2+}$ from 200 $\mu$M (+), to below 10 nM (−) in the bath solution, in a flash experiment (*a*) and in an experiment where light pulses were applied (*b*). The duration of the light pulse is indicated above the electrical traces ($K^+$ = 1 mM, pH 6.8). (*c* and *d*) Photocurrents recorded at different pH values at high $Ca^{2+}$ (200 $\mu$M (*c*)) and low $Ca^{2+}$ (< 10 nM (*d*)). Note that the time scale in *a* is different from that in *b–d*. Currents were filtered to 100 Hz (*b* and *c*) or 50 Hz (*d*) with a digital Gaussian filter.

The kinetics of $P_F$ remained stable, whereas the duration of $P_S$ was largely extended. To exclude the possibility that the currents are acid-facilitated $Ca^{2+}$ influxes, the experiments were repeated in the absence of $Ca^{2+}$ (Fig. 8 *d*). When the pH was changed from 6.8 to 4.1, the same dramatic increase in $P_S$ and $P_F$ reappeared, suggesting that both components are carried by $H^+$ under acidic conditions. In continuous light the $P_{St}$ amplitude was enlarged in a manner similar to that of $P_S$ in flash experiments (data not shown).

$P_F$, $P_S$, and $P_{St}$ differ from each other by their $K^+$ sensitivity. $P_F$ is independent of the extracellular $K^+$ concentration over a wide concentration range between 100 $\mu$M and 10 mM, provided the cells have adapted to the $K^+$ change. This observation is consistent with the interpretation that $P_F$ is not accompanied by significant $K^+$ efflux. The $K^+$ conductance, $G_K$, of the plasmalemma is low but not negligible (Malhotra and Glass, 1995). $P_S$ currents were unaffected by $K^+$ at pH 7 and low flash energies, but the high-energy responses were reduced by $K^+$. The enhanced $P_S$ currents recorded at pH 4 were reduced at elevated $K^+$ at all flash energies. $P_{St}$ currents completely disappeared at 10 mM $K^+$ (Fig. 9 *a*). These findings are consistent with a light-induced $K^+$ conductance, $G_K$. The $K^+$ efflux promotes $P_S$ and $P_{St}$ by stabilizing the membrane potential near $E_K$. The small positive current that continues beyond the duration of the light pulse at 10 mM $K^+$ (Fig. 9 *a*) is explained as a slightly unevenly distributed $K^+$ influx. At asymmetrical extracellular $K^+$ with 7 mM $K^+$ in the bath and 100 $\mu$M in the pipette, a transcellular $K^+$ flux is created. $K^+$ is directed through the activated $K^+$ conductance, $G_K$, from the bath into the cell and from the cell into the pipette (Nonnengässer et al., 1996). This transcellular $K^+$ flux is permanent in continuous light, whereas it is seen as a clearly defined peak that follows $P_F$ in flash experiments (Fig. 9 *b*). In *Chlamydomonas* $G_K$ is activated after the fast flagellar current (Govorunova et al., 1997), whereas in *Volvox* $G_K$ seems to be activated by the $P_F$-induced depolarization (Fig. 9 *b*).

## DISCUSSION

### Rhodopsin activation of the photoreceptor currents

The above-described experiments demonstrate in the spheroidal alga *Volvox carteri* the existence of photocurrents,

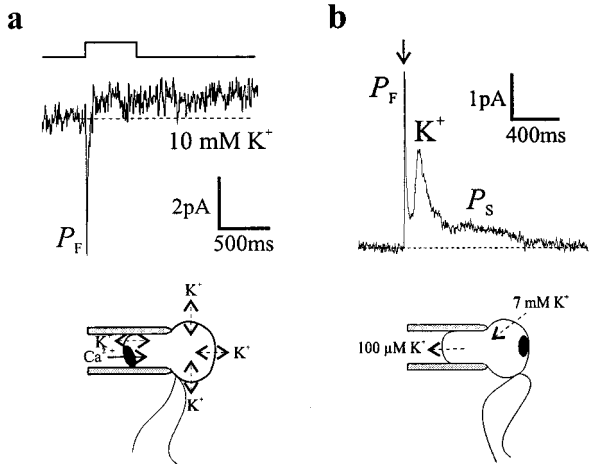


FIGURE 9 $K^+$ dependence. (*a*) Symmetrical high $K^+$ (10 mM) in bath and pipette abolishes the $K^+$ efflux, rendering $P_{St}$ undetectable as schematized in the inset (five averages, Gaussian filter 100 Hz). (*b*) Visualization of the $P_F$-triggered $K^+$ efflux at unsymmetrical extracellular $K^+$. The 7 mM $K^+$ in the bath solution and 100 $\mu$M in the pipette direct the $K^+$ into the pipette (average of 23 responses, 100 Hz Gauss).

which have all the characteristics needed to qualify them as the trigger for behavioral responses. The rhodopsin shape of the P-current action spectrum and its peak at 495 nm leave little doubt that the P-currents are triggered by rhodopsin. As already mentioned, the published action spectra for movement responses in colony-forming *Volvocaceae* all peak between 490 and 534 nm (Mast, 1917; Luntz, 1931; Halldal, 1958; Schletz, 1976; Sakaguchi and Iwasa, 1979). Reasons for the differences among the observed maxima are the different recording techniques and the intensities at which the responses were measured. In general, low-intensity action spectra for phototaxis, as well as the spectra for flash-induced phobic responses (flagellar arrest), peak at 490–500 nm and are rhodopsin shaped (Luntz, 1931; Schletz, 1976). They are in agreement with the photocurrent action spectrum of Fig. 3 *f*. The correlation supports the claim that the P-currents are the trigger for phobic responses and for phototaxis at low light. In contrast, high-intensity (finite response) phototaxis spectra are structured and red shifted by 20–30 nm. But these differences are explained by the photoreceptor optics, by shading pigments, by adaptation phenomena, and potentially by photoreceptor photochromism (Foster and Smyth, 1980; Hegemann and Harz, 1998). Thus the correlation between high-intensity action spectra and absorption of the rhodopsin is less accurate.

## Classification of the conductances

The major properties of the observed photocurrents are summarized in Table 1. Until now nothing was known about the visual process in multicellular *Volvocacean* algae such as *Volvox*, *Pandorina, Eudorina*, and other relatives. Only the availability of dissolver mutants made it possible to obtain information about the electrical processes. The *Volvox* spheroid rotates at 0.45 Hz (Gerisch, 1959; Schletz, 1976; Sakaguchi and Iwasa, 1979), which is slow compared to the 2 Hz rotation frequency of most unicellular flagellates (at room temperature). This explains why in *Volvox* all photocurrents are slower than in single-celled flagellates and why there is no need for a faster signaling system. One should keep in mind that a *Volvox* cell in nature always swims and navigates as part of a large spheroid and never as a single individual. The relatively slow P-current rise makes this alga a preferable model system for studying the rhodopsin-ion channel coupling in flagellate algae.

**TABLE 1 Classification of the photoreceptor currents in *Volvox***

| | $P_F$ current | $P_S$ current | $P_{St}$ current |
|---|---|---|---|
| Localization | Eyespot | Eyespot | Eyespot |
| Activated by | Rhodopsin | Messenger | Messenger |
| act. stimulus | Light flash | Light flash | Light pulse |
| Conducted ion | $Ca^{2+}$ ($H^+$) | $H^+$ | $H^+/Ca^{2+}$ |
| max. integral | 300 fC | 300 fC | — |
| Stationary current | — | — | 2–3 pA |
| Time range | 20–50 ms | 1000 ms | Permanent |
| Inactivation | Spontaneous | ? | Spontaneous |

The shape of the photoreceptor currents could be explained in at least three ways. First, the $P_S$ plateau is attributable to a desensitisation of the transduction mechanism; or, second, the current is limited by an outwardly directed countercurrent across the plasmalemma ($K^+$ efflux); or, finally, the transient $P_F$ and the slowly decaying $P_S$ reflect two independent conductances.

All *Volvox* photoreceptor currents (P-currents) are localized inward currents into the eyespot region, whereas the repolarizing $K^+$ efflux is more or less evenly distributed over the plasmalemma. The ion that carries the $P_F$ has not been unequivocally identified. But the sensitivity to extracellular $Ca^{2+}$, the maintenance of the conductance by $Ba^{2+}$, and its inhibition by $Ca^{2+}$ channel inhibitors are cumulative evidence that $P_F$ is mainly carried by $Ca^{2+}$. Neither the rapid response to external $Ca^{2+}$ nor the $Ba^{2+}$ substitution is compatible with the ideas that $Ca^{2+}$ only activates the channel from inside via $Ca^{2+}$ stores (Plieth et al., 1998) and that the channel conducts other ions but not $Ca^{2+}$. But the strong increase in the $P_F$ current at acidic pH without any change in the kinetics suggests that the underlaying conductance, $G_{Ca}$, conducts $H^+$ as well under selected conditions. In contrast, $P_S$ is quite obviously carried solely by $H^+$. A direct proportionality of the current amplitude to the extracellular $H^+$ concentration over a wide pH range is not expected, because the cell depolarizes during the $H^+$ influx and the $K^+$ efflux should become rate limiting at high $H^+$. Nevertheless, $P_F$ and $P_S$ must be mediated by two independent conductances, $G_{Ca}$ and $G_H$, similar to the two conductances in *Drosophila* eyes (Niemeyer et al., 1996).

Stationary photocurrents like $P_{St}$ were observed before in the unicellular flagellate *Haematococcus* (Sineshchekov, 1991), but the amplitude was small and the nature of this

current is unknown. The authors stated that the ion of the current is clearly not calcium, because it is not inhibited by $Ca^{2+}$ removal. In *Chlamydomonas* the stationary current is of similarly small size (Braun, unpublished observations). In *Volvox,* stationary P-currents are large, producing a massive cation influx during extended light pulses. The above experiments are consistent with a contribution of both conductaces $G_{Ca}$ and $G_H$ to $P_{St}$, at which $G_H$ is dominating under most conditions. The influx may reach $1 \times 10^7$ charges/s (at pH 7), corresponding to a total concentration increase of 10 $\mu$M $H^+$/s in a 15-$\mu$m cell.

A contribution of anions as $Cl^-$ to any of the photocurrents is electrically possible because the equilibrium potential for $Cl^-$ should always be positive, but so far there is no single experiment at hand that suggests an anion efflux.

## Channel activation

There are two photon exposure ranges that can be discriminated with respect to photocurrent activation. At the high intensity range above $10^{19}$ photons $m^{-2}$, the delay is below 50 $\mu$s. The extremely rapid activation of the P-current after a light flash in flagellate algae, first observed in *Haematococcus* (Sineshchekov et al., 1990), led to the suggestion of a direct coupling between rhodopsin and the ion channel (Harz et al., 1992). This close link was now confirmed in *Volvox*. However, the hypothesis remained controversial because in all former studies the peak amplitude was analyzed and the light dependence did not follow a monoexponential function (Sineshchekov, 1991; Harz et al., 1992; Beck, 1996). The use of pipettes with steep cone angle now improved the resolution and made it possible to study on one hand photocurrents in response to very low flash energies, and on the other hand to analyze the P-current initial rise. The saturation of the rise follows a single exponent, as expected for a fixed coupling between rhodopsin and the channel. A linear signal chain explains the sigmoidicity of the rise if the light-excited rhodopsin activates the channel via at least one intermediate state:

$$Rh \rightarrow Rh^* \rightarrow I \rightarrow G_{Ca}$$

This intermediate state, I, may be an intermediate of the rhodopsin photocycle, a separate transmitter compound, a separate state of the channel, or, finally, a state of a common rhodopsin-ion channel complex. However, in contrast to a signaling system with dynamic amplification, a linear model with fixed decay rates cannot explain the light dependence of the delay between flash and P-current rise (Gradmann and Hegemann, unpublished observations).

The flat slope of the stimulus-response curve for the peak current was explained for *Chlamydomonas* by the depolarization during the response. This depolarization accelerates the current decay, shifts the peak to shorter times, and reduces the current size at high flash energies (Harz et al., 1992). In vertebrate vision, flash-induced currents are quite independent of the voltage changes occurring during a flash response (Bader et al., 1979), but nevertheless the influence of voltage changes is visible (Lamb et al., 1981). However, depolarization does not explain the flat dose-response curve for peak currents in *Volvox*. Here the $P_F$ decay is independent of the current size, which would not be the case if the peak current were reduced by the progressing depolarization. Second, because of the slow decay, at peak the current integral reached only 10% of the total. In a *Volvox* cell 15 $\mu$m in diameter, P-currents with integrals of up to 300 fC should lead to a depolarization of ~50 mV (for a detailed explanation see Harz et al., 1992). Thus the depolarization is only 5 mV at peak and cannot explain a strong size reduction at high flash energies due to voltage inactivation.

The exponential saturation curve of the P-current rise and its close fit by the numerical calculation based on typical rhodopsin values implicates that the $P_F$ rise is directly proportional to the amount of rhodopsin bleached by the flash. It is also compatible with the earlier presented model that the rhodopsin and the primary channel form a single protein complex. However, the nonexponential saturation curve for the total peak current, the biphasic current decay with a light dependent ratio of $\tau_1/\tau_2$, and the different ion dependence of $P_F$ and $P_S$ are, taken together, only explained by two signaling systems as they are schematized in Fig. 10. A saturating flash of $4-8 \times 10^{20}$ photons $m^{-2}$ bleaches practically all rhodopsin molecules of the cell. The bleached photoreceptors undergo a transition to the signaling state, from which they activate by direct contact a cation conductance, $G_{Ca}$, in the eyespot overlaying part of the plasmalemma. It conducts mostly $Ca^{2+}$ under physiological conditions. The activation occurs in the submillisecond range and is faster than ion channel activation in any animal visual system. The $Ca^{2+}$ influx reaches its maximum after 2.5–3 ms. Under all conditions the $P_F$ current of a particular cell decays with the same time constant. Hence the decay rate is an intrinsic property of the channel. Second, rhodopsin induces a long-lasting inward current of only 1 pA. This $P_S$ current is carried by $H^+$. $P_S$ is activated with a delay of up to 10 ms and peaks after 2.5–25 ms. The responsible channel is not directly activated by rhodopsin but rather via a signal amplification system, which is likely to include a G-protein. The conductance $G_H$ saturates when only a few percent of the rhodopsin is bleached.

Because of the chlamyopsin sequence, which predicts a highly charged protein with some sequence homology to $K^+$ channels, we had suggested that chlamyrhodopsin is part of a rhodopsin-ion channel complex or even forms a channel by itself, or, in other words, it constitutes a channel with an intrinsic light sensor. The volvoxopsin is up to 62% identical to chlamyopsin and certainly belongs to the same gene family. It exhibits very similar features and should fulfill the same role. On the other hand, if only one type of rhodopsin exists in green algae as concluded by biochemical experiments (Kröger and Hegemann, 1994), the rhodopsins must also function as a remote sensor activating $P_S$ via an amplification system. Despite these needs, there are no

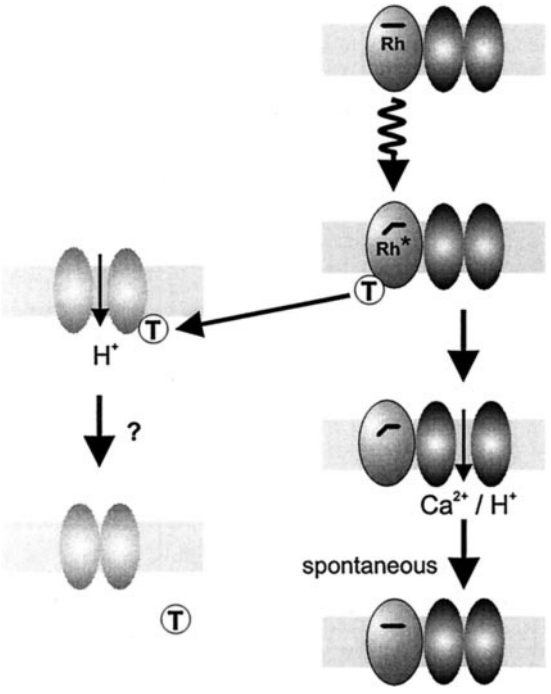


FIGURE 10 Model of rhodopsin-triggered conductances. Upon flash stimulation light-excited rhodopsin, Rh*, activates two conductances, $G_{Ca}$ and $G_H$, $G_{Ca}$ by direct contact and $G_H$ most likely via a transducer (T), which could be a G-protein. The corresponding channels $PC_{Ca}$ and $PC_H$ are localized within the eyespot area. $PC_{Ca}$ inactivates spontaneously and independently of the extracellular $Ca^{2+}$ concentration and the actual membrane potential. The inactivation of $PC_H$ is unclear, but most likely is brought about by the decay of the messenger. In continuous light, both $G_{Ca}$ and $G_H$ in combination with a nonlocalized K conductance, $G_K$, constitute the stationary current $P_{St}$.

evident G-protein-binding domains in the algal opsin sequences (Ebnet et al., manuscript submitted for publication). However, Kreimer and colleagues identified a G-protein in eyespot fractions of the green alga *S. similis*. Its GTPase acitivity is light dependent and is sensitive to anti-chlamyopsin antibodies (Calenberg et al., 1998). Thus this G-protein is an appropriate candidate for enabling rhodopsin-triggered remote sensing in green algae. G-protein activation and the downstream ion channel modulation occur in animal vision within the expected time scale of 2.5–25 ms (Felber et al., 1996), which is the time scale observed for the $P_S$ delay.

## Physiological implications

It is now abundantly clear that in *Chlamydomonas* as in other eucaryotes from ciliates to mammals, flagellar activity is regulated by the $Ca^{2+}$ level in the cytoplasm (Tamm, 1994). It is also accepted that a $Ca^{2+}$ ATPase operates continuously to keep the $Ca^{2+}$ concentration at a submicromolar level. But from the presented data it is clear now that in green algae during the continuous photocurrents, $Ca^{2+}$ only accompanies monovalent ions as in animal visual processes, but may fulfill its physiological role as the key control element for flagellar beating (Witman, 1994; Holland et al., 1997) without any restriction.

$Ca^{2+}$ is a favorable ion for carrying the $P_F$ because in dark-adapted *Volvox* cells $Ca^{2+}$ is under a higher driving force. The intracellular $Ca^{2+}$ is in the range of 100 nM (M. Fischer, unpublished) and between 0.1 and 0.3 mM in the growth medium and in the bath during experiments. On the other hand, high cytoplasmic $Ca^{2+}$ levels would be harmful. Thus it is more beneficial for the alga if $Ca^{2+}$ plays a modulating role in continuous light, and $H^+$ instead of $Ca^{2+}$ is used as the major current carrier. However, the $H^+$ gradient is relatively small at pH 7 (below 1 log unit at pH 7; Malhotra and Glass, 1995; Fischer and Braun, unpublished), and the amplitude is accordingly small. At higher pH gradients the driving force for $H^+$ is increased, but the $H^+$ influx is only maintained if it is accompanied by the $K^+$ efflux.

The finding that the photoreceptor currents increase with the photon exposure until all of the rhodopsin is bleached provides new perspectives for the control of the flagella that execute the response. If the flagellar beat frequency is controlled in *Volvox* by the membrane potential, by a proton influx, and by $Ca^{2+}$, beating should be modulated over a broad range of photon exposure. Unfortunately, this has not been tested so far. But beating in response to step-up stimulation was measured by video microscopy (reviewed by Hoops, 1997). As expected, the beating was reduced almost to zero and recovered to a stationary level after one or two seconds. The transient frequency reduction is larger compared to that of *Chlamydomonas* or other single-celled algae. But single-celled species compensate for that deficit with the ability to perform phobic responses (flagellar reprogramming). These shock responses are caused by an action potential-like fast flagellar current, $F_F$, which causes a massive $Ca^{2+}$ influx along the whole flagellar length, thus triggering backward swimming for some hundred milliseconds (Litvin et al., 1978; Harz and Hegemann 1991; Beck and Uhl, 1994; Holland et al., 1997). This type of response and consequently the $F_F$ current are totally absent in *Volvox*. Backward swimming makes no sense for an alga that is part of a large colony of several thousand individuals. $Ca^{2+}$ is expected to modulate the flagellar beat frequency by acting only at the flagellar basis (on-off response; Tamm, 1994). This may happen in two ways: either there are $Ca^{2+}$ channels restricted to the flagellar base, which have a conductance too low to be seen in our experiments, or $Ca^{2+}$ diffuses from a cytosolic source to the flagella.

We thank Markus Fischer for his skillful assistance during the electrical measurements. We thank Dr. Dieter Gradmann for his critical and stimulating comments and Dr. D. Kirk for providing the mutant W251, which was a *conditio sine qua non* for this work.

This project was supported by the Deutsche Forschungsgemeinschaft and the Fond der Chemischen Industrie.

## REFERENCES


Bader, C. R., P. R. MacLeish, and E. A. Schwarz. 1979. A voltage clamp study of the light response in solitary rods of tiger salamander. *J. Physiol. (Lond.).* 296:1–26.

Beck, C. 1996 Lokalisation und Eigenschaften lichtinduzierter Ionenströme in *Chlamydomonas reinhardtii.* Thesis. Universtät München.

Beck, C., and R. Uhl. 1994. On the location of voltage sensitive calcium channels in the flagella of *Chlamydomonas*. *J. Cell Biol.* 125: 1119–1125.

Calenberg, M., U. Brohsonn, M. Zedlacher, and G. Kreimer. 1998. Light and $Ca^{2+}$ modulated heterotrimeric GTPases in the eyespot apparatusses of flagellate green algae, the photoreceptive organells for phototaxis and photoshock. *Plant Cell.* 10:91–103.

Deininger, W., P. Kröger, U. Hegemann, F. Lottspeich, and P. Hegemann. 1995. Chlamyrhodopsin represents a new type of sensory photoreceptor. *EMBO J.* 14:5849–5858.

Felber, S., H. P. Bauer, F. Petroccione, J. Honerkamp, and K. P. Hofmann. 1996. Stochastic simulation of the transducin GTPase cycle. *Biophys. J.* 71:3051–3063.

Foster, K. W., and R. D. Smyth. 1980. Light antennas in phototactic algae. *Microbiol. Rev.* 44:572–630.

Gerisch, G. 1959. Die Zelldifferenzierung bei *Pleodorina californica Shaw* und die Organisation der Phytomonadenkolonien. *Arch. Protistenkunde.* 104:292–358.

Govorunova, E. G., O. A. Sineshchekov, and P. Hegemann. 1997. Desensitisation and dark recovery of the photoreceptor current in *Chlamydomonas. Plant Physiol.* 115:633–642.

Halldal, P. 1958. Action spectra of phototaxis and related problems in *Volvocales*, *Ulva* gametes and *Dinophyceae. Physiol. Plant.* 11: 118–153.

Harz, H., and P. Hegemann. 1991. Rhodopsin-regulated calcium currents in *Chlamydomonas. Nature.* 351:489–491.

Harz, H., C. Nonnengässer, and P. Hegemann. 1992. The photoreceptor current of the green alga *Chlamydomonas. Philos. Trans. R. Soc. Lond. Biol.* 338:39–52.

Hegemann, P., and H. Harz. 1998. How microalgae see the light. *In* Microbial Responses to Light and Time. Society for General Microbiology Symposium. M. X. Caddick, S. Baumberg, D. A. Hodgson, and M. K. Phillip-Jones, editors. Cambridge University Press, Cambridge. 95–105.

Holland, E-M., F.-J. Braun, C. Nonnengässer, H. Harz, and P. Hegemann. 1996. The nature of rhodopsin triggered photocurrents in *Chlamydomonas.* I. Kinetics and influence of divalent ions. *Biophys. J.* 70:924–931.

Holland, E.-M., H. Harz, R. Uhl, and P. Hegemann. 1997. Control of phobic behavioural responses by rhodopsin-induced photocurrents in *Chlamydomonas. Biophys. J.* 73:1395–1401.

Hoops, J. H. 1993. Flagellar, cellular and organismal polarity in *Volvox carteri. J. Cell Sci.* 104:105–117.

Hoops, J. H. 1997. Motility in the colonial and multicellular *Volvocales*: structure, function and evolution. *Protoplasma.* 199:99–112.

Kirk, D. L., R. Birchem, and N. King. 1986. The extracellular matrix of *Volvox*: a comparative study and proposed system of nomenclature. *J. Cell Sci.* 80:207–231.

Kirk, D. L., and J. F. Harper. 1986. Genetic, biochemical and molecular approaches to *Volvox* development and evolution. *Int. Rev. Cytol.* 99: 217–293.

Kirk, D. L., M. R. Kaufman, R. M. Keeling, and K. A. Stamer. 1991. Genetic and cytological control of the asymmetric divisions that pattern the *Volvox* embryo. *Dev. Suppl.* 1:67–82.

Kröger, P., and P. Hegemann. 1994. Photophobic responses and phototaxis in *Chlamydomonas* are triggered by a single rhodopsin photoreceptor. *FEBS Lett.* 341:5–9.

Lamb, T. D., P. A. McNaughton, and K.-W. Yau. 1981. Spatial spread of activation and background desensitisation in toad rod outer segments. *J. Physiol. (Lond.).* 319:463–496.

Litvin, F. F., O. A. Sineshchekov, and V. A. Sineshchekov. 1978. Photoreceptor electric potential in the phototaxis of the alga *Haematococcus pluvialis. Nature.* 271:476–478.

Luntz, A. 1931. Untersuchungen über die Phototaxis. I. Mitteilung: die absoluten Schwellenwerte und die relative Wirksamkeit von Spektralfarben bei grünen und farblosen Einzellern. *Z. Vergl. Physiol.* 14:68–92.

Malhotra, B., and A. D. M. Glass. 1995. Potassium fluxes in *Chlamydomonas reinhardtii. Plant Physiol.* 108:1527–1536.

Mast, S. O. 1917. The relation between spatial color and stimulation in the lower organism. *J. Exp. Zool.* 22:471–528.

Niemeyer, B. A., E. Suzuki, K. Scott, K. Jalink, and C. S. Zuker. 1996. The *Drosophila* light-activated conductance is composed of two channels TRP and TRPL. *Cell.* 85:651–659.

Nonnengässer, C., E. M. Holland, H. Harz, and P. Hegemann. 1996. The nature of rhodopsin triggered photocurrents in *Chlamydomonas*. II. Influence of monovalent ions. *Biophys. J.* 70:932–938.

Plieth, C., B. Sattelmacher, U.-P. Hansen, and G. Thiel. 1998. The action potential in *Chara*: $Ca^{2+}$ release from internal stores visualized by $Mn^{2+}$-induced quenching of fura-dextran. *Plant J.* 13:167–175.

Provasoli, L., and I. J. Pinter. 1959. Artificial media for freshwater algae: problems and suggestions. *In* The Ecology of Algae, Special Publication no. 2. C. A. Tyron and R. T. Hartman, editors. Pymatuning Laboratory of Field Biology, University of Pittsburgh. 84–96.

Sakaguchi, H., and K. Iwasa. 1979. Two photophobic responses in *Volvox carteri. Plant Cell Physiol.* 20:909–916.

Schletz, K. 1976. Phototaxis bei *Volvox*. Pigmentsysteme der Lichtrichtungsperzeption. *Z. Pflanzenphysiol.* 77:189–211.

Sineshchekov, O. A. 1991. Photoreception in unicellular flagellates: bioelectric phenomena in phototaxis. *In* Light in Biology and Medicine, Vol. 2. R. H. Douglas, editor. Plenum Press, New York. 523–532.

Sineshchekov, O. A., F. F. Litvin, and L. Keszethely. 1990. Two components of the photoreceptor potential in phototaxis of the flagellated green alga *Haematococcus pluvialis. Biophys. J.* 57:33–39.

Smyth, R. D., J. Saranak, and K. W. Foster. 1988. Algal visual systems and their photoreceptor pigments. *Prog. Phycol. Res.* 6:255–286.

Tam, L.-W., and D. L. Kirk. 1991. The program for cellular differentiation in *Volvox carteri* as revealed by molecular analysis of development in a gonidialess/somatic regenerator mutant. *Development.* 112:571–580.

Tamm, S. 1994. $Ca^{2+}$ channels and signalling in cilia and flagella. *Trends Cell Biol.* 4:305–310.

Witman, G. B. 1994. *Chlamydomonas* phototaxis. *Trends Cell Biol.* 3:403–408.